



Chapter 1: Introduction

1.1. GENERAL INTRODUCTION

Zeolites are microporous material which have added new horizon in the material science and grabbed the attention of researchers in the modern time period. The material has special type of lattice architecture and provides a very convenient route for the various types of applications in catalysis, petrochemical industry, and in various large-scale industrial processes since zeolites have significant thermal stability, chemically robustness, ease in separation from reaction media and reusability without any loss of activity.¹⁻⁴ The zeolites have shown great success as catalysts in several gas or solution phase reactions and employed for the development catalytic progression for the production of the fine chemicals.⁵⁻⁷ These materials are sometimes better choice in the place of the solvents as reaction medium and offer the environment benign course for the different organic transformations. In addition to that, the architecture of zeolite material provides a convenient way of heterogenization of the homogeneous catalyst to couple their reactivity with the additional advantages provided by the specific environment and architecture of host material.^{3, 7-9} These contemporary classes of catalysts can afford an exclusive approach to encapsulate the single-site catalyst molecule within the well ordered cavities of the host, having large surface area. These systems are well known mimic of biological systems and have shown structural and functional analogy with the cytochrome P-450 and termed as zeozymes.¹⁰⁻¹³ A variety of organometallics, transition complexes, organic molecules and dyes have been encapsulated in the zeolites and these “hybrid systems” have shown the profound modified reactivity for the various transformations.^{8, 13-19} The reusability of such systems also economical proficient processes as many transition metal complexes are expensive and non-reusable in their homogeneous states, however after encapsulation within the zeolites they are reusable for many times with the comparable reactivity. Furthermore, the rigid walls of material induce space constraint on the encapsulated transition complex and the topology imposes noticeable change in the spectroscopic, redox and magnetic behavior of the guest complex²⁰⁻²³. As the result, encapsulated complex exhibits the modified chemical reactivity in comparison of its homogeneous counterpart. It quite significant to investigate the influence of the topology of framework on the geometry of guest complex phthalocyanines,¹³ porphyrins²⁴ and salen metal complexes²⁴ are extensively studied in the encapsulated state in microporous and

mesoporous host materials and have been identified as eminent potential biomimetic catalysts for the various oxidation processes.

This thesis deals with the encapsulations of square-planar Co (II), Ni (II), Cu (II) and Pd (II) Schiff base complexes within the zeolite-Y. Encapsulation of transition metal Schiff base complexes within the voids of microporous materials have been in immense attention for the recent decade. These Schiff-base complexes of transition metals are so chosen that they have end-to-end dimension comparable with the diameter of nearly spherical supercage of zeolite Y and can be encapsulated in the host framework. In the present work we have synthesized metal complexes with different molecular dimensions following the increasing order of the molecular dimension and well characterized by electronic (UV-Vis) and vibrational (IR) spectroscopic studies, X-ray diffraction methods, scanning electron microscopy (SEM-EDX), X-ray photo electron spectroscopy (XPS), magnetic susceptibility measurements and theoretical studies and also employed as catalysts for the catalytic oxidation reactions. Transition metal (Ni, Co, Cu and Pd) complexes of Schiff-base ligands with general formula: *N,N'*-bis(salicylidene)ethylenediamine (L1), *N,N'*-bis(4-hydroxy-salicylidene)ethylenediamine (L2), *N,N'*-bis(5-hydroxy-salicylidene)ethylenediamine (L3), *N,N'*-bis(5-bromo-salicylidene)ethylenediamine (L4), *N,N'*-bis(5-methyl-salicylidene)ethylenediamine (L5) and *N,N'*-bis(5-methoxy-salicylidene)ethylenediamine (L6) (Given in Figure 1.13) have been synthesized *via flexible ligand synthesis method* to form so-called *ship-in-a-bottle* complexes. In the following section these aspects of the present study are discussed.

- c Zeolites: structure and composition.
- c Heterogenization of transition metal complexes.
- c Catalytic application of zeolite Y encapsulated complexes.
- c Spectroscopic, physiochemical characterization and theoretical studies to understand the adopted geometry under encapsulation.

1.1.1. ZEOLITES: STRUCTURE AND COMPOSITION

Zeolites are the three dimensional crystalline aluminosilicate microporous materials,²⁵ and often referred as inorganic polymers (Figure. 1.1 and 1.2). The material consists of SiO_4^{4-} and AlO_4^{5-} tetrahedral units,²⁶ which are the basic building blocks (BBU) of the framework, and connected through sharing the oxygen atom as the corner.²⁷ Generally these units can be

represented as TO_4 where T stands for tetrahedral units; though the T-O-T angle is not perfect tetrahedral angle. In fact it lies within the range of $140\text{--}160^\circ$. To maintain the charge neutrality of the mono-valent extra-framework ions like sodium ions reside in the cavities and channels of the material. These Na^+ ions are exchangeable with other mono and divalent cations, such as alkali, ammonium and transition metal ions etc. The Si atom is replaced by isomorphic Al atoms and it is a characteristic property of these materials which can be represented in terms of the Si/Al ratio. According to Löwenstein rule, aluminium atom must be surrounded by four tetrahedral SiO_4^{4-} units as Al-O-Al linkages are prohibited in the network.²⁸ In general Löwenstein rule is followed by the zeolites framework however recent reports have depicted the presence of non Löwenstein arrangements of AlO_4^{5-} units also at high temperature in zeolitic network.²⁹ The structural and chemical aspects of the material are determined by the number of tetrahedral units, oxygen and Si/Al ratio, and these factors distinguish the materials with ultra large, large, medium and small pores.³⁰ The secondary building units (SBU) can be formed by the linked up of 16 basic building blocks and these SBU are interconnected and form the hollow 3D network.³¹ These contain condensed octahedra β cage composed by 4 and 6 rings and α cage is formed by interconnecting 8 rings. Zeolite Y is also belongs to this class of materials and it shows the FAU (faujasite) structure.³¹

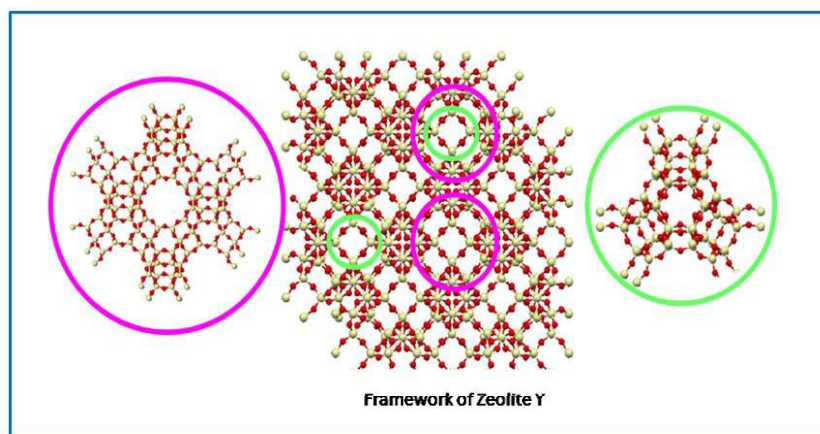


Figure 1.1: Structure of zeolite Y.

The supercages are comparatively large, open and connected to four other supercages by windows of $\sim 8\text{\AA}$ diameter. Similarly sodalite cages are also connected to the supercages through eight sided double windows which are narrower (diameter $\sim 5\text{\AA}$). There are eight supercages per unit cell in the zeolite-Y framework with the Si/Al ratio = 2 to 5.^{32, 33}

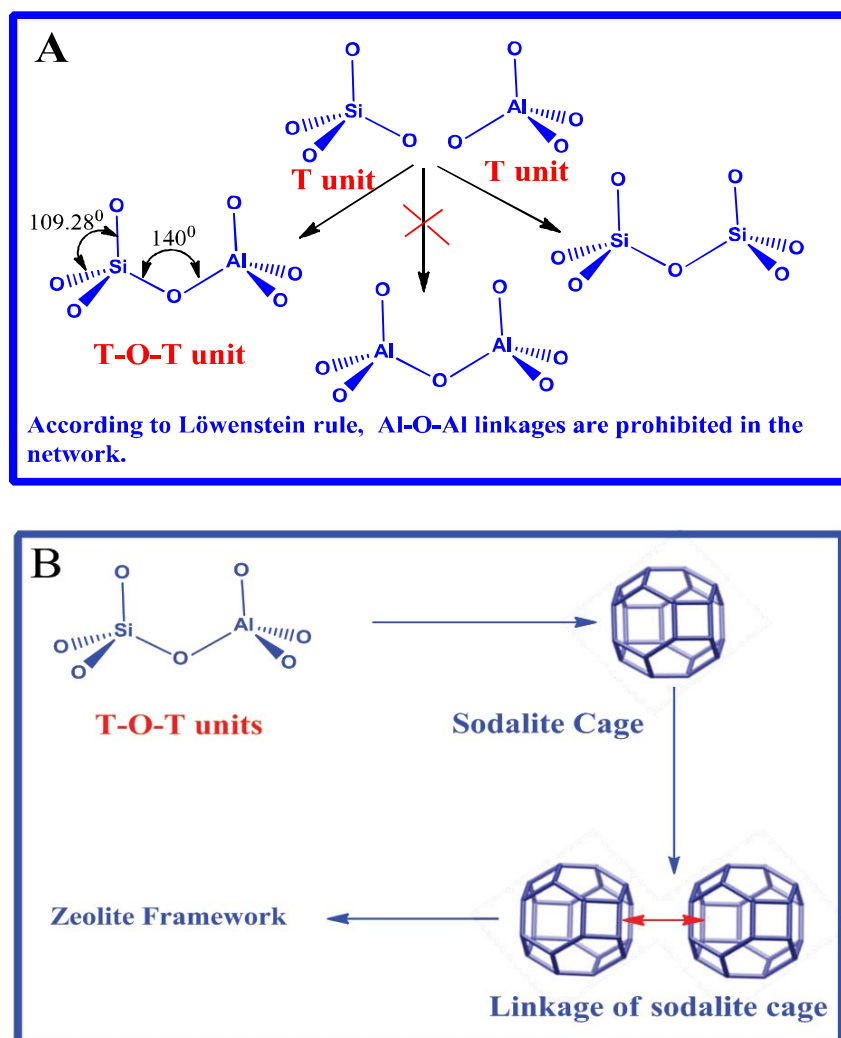


Figure 1.2: (A) Basic building blocks of zeolite framework, (B) Linkage between sodalite cage and supercage of zeolite-Y.

1.1.2. Heterogenisation of Transition Metal Complexes (Ship-in-Bottle Complexes)

Zeolite Y has a microporous framework and it consists of windows, channels and cavities of precise size and shape. This beautiful architecture of the material allows to diffuse the small molecules at the surface as well as inside the cavities of framework. Such unique structural characteristic of the material makes it suitable host material for the various organic molecules and organometallics and this process is known as encapsulation. Metal-Salen [N, N' - bis(salicylaldehyde)ethylenediimine], metal tris(bipyridyl), metallophthalocyanine (MPC), metalloporphyrins encapsulated in zeolite-Y are important examples of *ship-in-a-bottle* complexes.^{34, 35} The molecular dimensions of these complexes are comparable with that of

the supercage, but far exceed that of the entrance to the supercage (7.4Å). These complexes, consequently, have to be assembled *in-situ* by taking the metal-ion and ligand together inside the zeolite cage. Once synthesized, the complex cannot be removed without destroying the host framework. When the molecular dimension of the complex is comparable or slightly larger than that of the zeolite, the structure of the encapsulated complex is expected to differ from that of its ‘unencapsulated’ or ‘free’ state. The size and topology of zeolite cage would have a profound influence on the geometry that a complex adopts on encapsulation. Small distortion in the geometry from that in the ‘free’ or unencapsulated state could in turn lead to profound changes in the electronic and magnetic properties, as well as, functionality of the encapsulated complex from its ‘free’ state. Thus the complexes in the ‘hybrid systems’ are attractive especially in terms of their modified functional behavior and its consequences.

1.1.3. Design of Heterogeneous catalyst

There are essentially three different synthetic approaches for synthesis of zeolite encapsulated metal complexes:

- i. Reaction of a synthesized ligand, with the transition metal ion which is already introduced into the zeolite cages (**flexible ligand method**).
- ii. Assembling the ligand around a metal ion, from smaller species, inside the zeolite cavity (**template synthesis method**).
- iii. Synthesis of the zeolite framework around a synthesized transition metal complex (**zeolite synthesis method**).

1.1.3.1. Flexible ligand method

This methodology is the most common and extensively used for the synthesis of a particular type of hybrid systems, where ligand are flexible in nature and has comparable size with the dimension of zeolite supercage, e.g., Schiff bases.^{24, 36} In this approach, transition metal ions are introduced by the method of ion-exchange into the zeolite. In this method desired transition metal ion is exchanged with sodium ions of zeolite framework by the help of ion exchange reaction. This exchange reaction is an essential step for the ‘flexible ligand synthesis’ or ‘template method’ for the synthesis of various zeolite embedded complexes. For this procedure, pure Na-zeolite Y is allowed to be dispersed in the desired metal salt solution to acquire required loading level of metal ions, and stirred at room temperature for 24 hours.

The slurry is filtered, washed frequently with the deionised water and further desiccated for one to two days at 150°C. After ion exchange procedure a flexible ligand is then allowed to diffuse freely through the zeolite pores while heating the reaction mixture within the range of 150-250°C for 24-48 hours reaction time. The ligand on encountering a transition metal ion, within a supercage reacts and forms the encapsulated complex (Figure 1.3A). The synthesized complex is subjected to extraction with the different solvents in sequence as acetone, methanol, and finally diethyl ether to remove the excess ligand which remains unreacted during the encapsulation process.^{36,37} The final products are dried in a muffle furnace for 10-12 hours at 150°C. Recovered material is further reacted with NaCl solution for 12 hours to remove the unreacted metal ions, followed by filtration and washing until the filtrate has negative test for chloride ions. The resulting complex is too large to escape through the windows and is trapped within the supercage. This approach is well suited for the encapsulation of metal-salen complexes, since the salen ligand offers the desired flexibility. The thermal stability of the ligand play an important role in this procedure as the ligand should not be decomposed at the reaction temperature. The free salen ligand enters into the supercage through the windows connected to it; diffusion becomes easier possibly because of the free rotation around the carbon-carbon σ -bond connecting two salicylidene moieties. However once chelated, with the exchanged transition metal ion inside, the ligand loses its flexibility. The fixed specific geometry of the complex does not allow it to leak out through the windows connected to the supercage of the host matrix since the molecular dimensions of complex is much bigger than that of its windows. This method is first reported by Herron for the synthesis of cobalt salen complexes in zeolite Y.³⁵ Subsequently, the procedure has been employed for the encapsulation of different transition metal complexes, such as Schiff-base complexes of cobalt,³⁵ nickel,³⁸ copper,³⁹ iron,¹⁸ manganese,³⁷ palladium,⁴⁰ vanadium,³⁹ and zinc³⁸ in zeolite Y.

1.1.3.2. Template Method

This method is basically applied when the molecular dimensions of ligands are bigger than the diameter of pores connected to the supercage hence diffusion of ligand through the pore is not viable. In such cases the precursors molecules or the building blocks of ligands are introduced in the metal exchanged zeolite cage where '*in situ*' complex formation takes place. This approach has been extensively used to encapsulate transition metal-tris(bipyridyl)

complex ion, metallophthalocyanine and metalloporphyrins complexes within zeolites (Figure 1.3B). For instance, to synthesize tris(bipyridyl) complex inside the supercage of zeolite-Y, the building block of the ligand, bipyridine is allowed to diffuse through. M(II)-tris(bipyridyl) complex ions was first reported by Mizuno and Lunsford.⁴¹ In case of phthalocyanine, the building blocks are 1, 2 dicyanobenzene. The synthesis of the phthalocyanine metal complexes, final step involves reduction of the phthalocyanine precursor for which the zeolitic water plays a crucial role supplying the electron. Thus synthesis of encapsulated phthalocyanine metal complex in zeolite, it is necessary the zeolite should not be fully dehydrated before the reaction. This approach has been used to prepare different encapsulated phthalocyanine complexes e.g., cobalt,^{22, 42, 43} nickel,⁴² copper,⁴⁴ iron,³⁴ ruthenium⁴⁵ and rhodium⁴⁶ phthalocyanines inside zeolite-Y.

1.1.3.3. Zeolite Synthesis Method

A more recent method for encapsulating metal complexes in zeolite, is the zeolite synthesis method. In this approach, the metal complex which is to be encapsulated is added during the crystallization of the zeolite (Figure 1.3C), so that crystallization of zeolite happens around the metal complex. This is another template synthesis type approach where the complex perhaps acts as a template and is eventually trapped within the zeolite. The zeolite can be synthesized with the help of the silica source which is dissolved in sodium hydroxide solution. The desired metal complex is added stirred for 30 minutes. Aluminium isopropoxide, which is dissolved in sodium hydroxide, is added and the resulting gel is autoclaved at 363 K for 24 hours then Soxhlet extracted.

It is essentially required that the complex should be adequate soluble in the zeolite synthesis medium as well as it must have good thermal, pH and temperature resistivity to accomplish the process. This is a method where building of a ‘bottle’ around the ‘ship’ takes place, the necessary condition is that the presence of the complex should not alter the windows of the framework. Balkus and co-workers have encapsulated the transition metal complexes of Co(II) and Cu(II) perfluorophthalocyanine by synthesizing the zeolites (X and Y) around the complex.⁴⁷ K. J. Balkus and co-workers have claimed that homogeneous encapsulation of the transition metal complexes in zeolite is possible by careful design of the zeolite synthesis procedure to avoid the aggregation of the complex molecules in the aqueous synthesis medium.⁴⁸ Encapsulation of phthalocyanine, porphyrins and amino acids complexes is carried

out by this procedure. This method has advantages that only distinct metal complexes, which do not have contamination of excess ligands or uncomplexed metal ions, can be synthesized in this way.

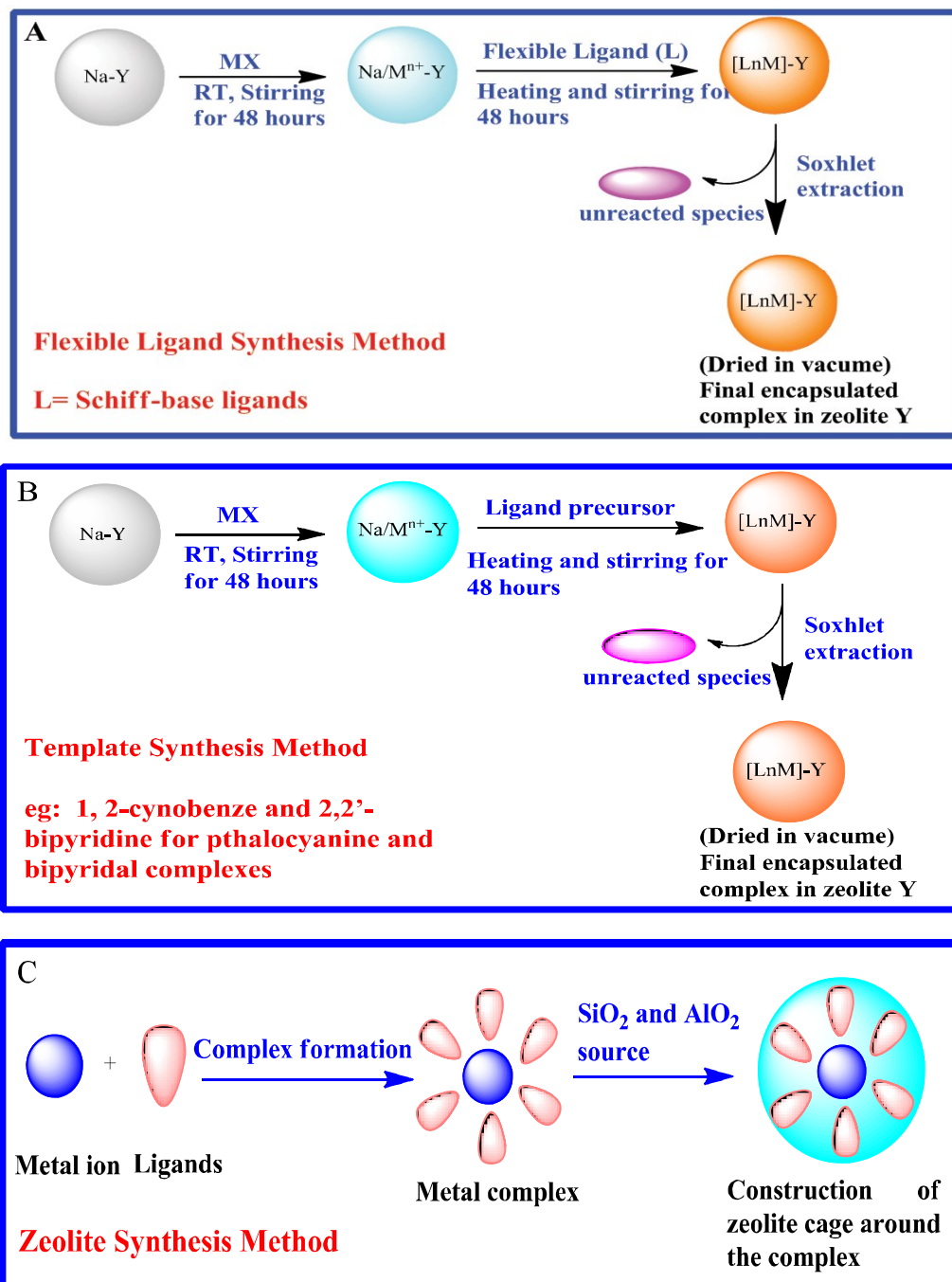


Figure 1.3: Different approaches for the synthesis of metal complex inside the cavity of zeolite Y. (A) Flexible ligand (B) Template synthesis method and (C) Zeolite synthesis method.

1.2. Zeolite Encapsulated Metal Complexes: As Catalysts

Transition metal complexes in encapsulated state in zeolite are identified as potential heterogeneous catalysts in various catalytic processes, like photo catalysts, redox catalysts, sensors, catalysts for asymmetric synthesis and oxidation. Such ‘hybrid’ systems are distinguished or well explored as oxidation catalysts and often termed as ‘zeozymes’.²⁴ The origin of the word ‘zeozymes’ is from the fact that such zeolite encapsulated hybrid system closely mimic some of the enzymes are considered as ‘synthetic enzymes’ due to their structural along with functional analogy with the biological enzymes (Figure 1.4). The 3D framework of the zeolite having windows and channels with precise size and shape can be considered as rigid analogues of the protein cavities of natural enzymes with the zeolite structure providing the steric selectivity. The aspiration to mimic enzymatic systems has prompted into an extensive area of research of encapsulated porphyrins, phthalocyanine and Schiff-base models of enzyme active sites, especially as models or synthetic analogues of the monooxygenase enzymes belonging to the cytochrome P-450 family.

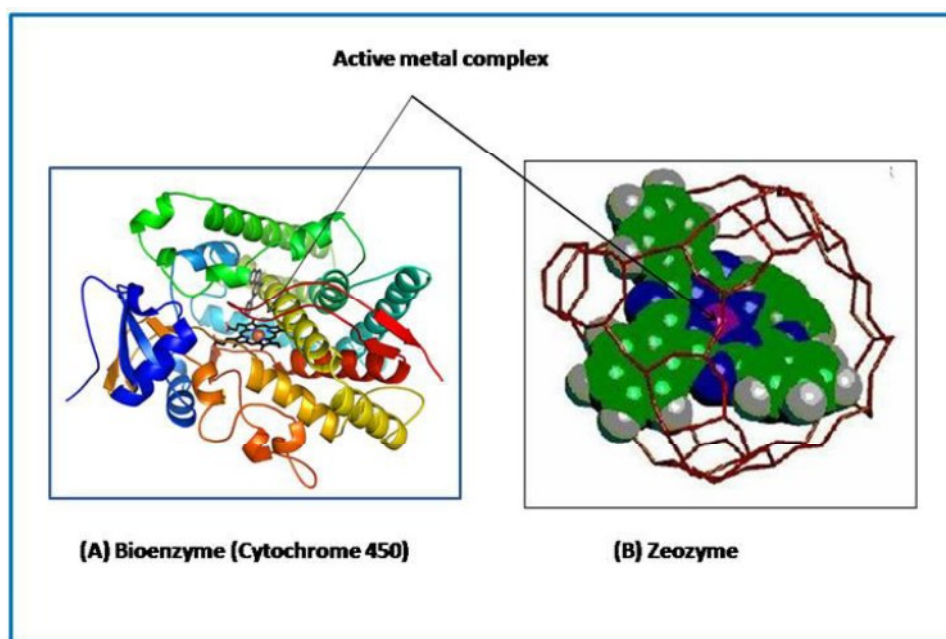


Figure 1.4: (A) Cytochrome P- 450 bioenzymes. (B) Co (II) phthalocyanine complex inside zeolite-Y (adapted from ref. 22) (zeozyme)

It is well established that the transition metal complexes of phthalocyanine, porphyrins and Schiff-base ligands are proficient catalysts for the various oxidation processes like oxidation

of phenols, alcohols, carbonyl compounds, alkenes and carboxylic acids; these are essential reactions in organic synthesis. In conventional synthetic route, the homogeneous catalyst are also effective for such processes in mild reaction condition and but they have some limitations in terms of stability, deactivation of catalyst due to aggregation or dimer formation, difficulty in separation from reaction medium and lack of reusability etc. These difficulties have been conquered by encapsulating these metal complexes within the larger cavities of zeolite X and Y which actually adds the special environment for catalysis provided by the host framework, while the guest molecule occupies the host cavity singly. In addition, the complex in encapsulated state largely shows altered functionality in terms of enhanced reactivity or better selectivity. The advantages of the encapsulation undeniably have grabbed the attention of researchers for last few decades so that the altered functionality can be explored to design innovative and attractive catalysts designed for the various organic transformations. Table 1.1, 1.2 and 1.3 summarizes the catalytic activity of zeolite encapsulated metal-phthalocyanine, porphyrins complexes, bipyridyl, amino acids and Schiff-base complexes.

Table 1.1: Catalytic activity of zeolite encapsulated metal-phthalocyanine and porphyrins complexes.

S.No	Encapsulated Complex	Reaction/References
1.	Fe Phthalocyanine in zeolite-Y	Preferential oxidation of tertiary C-H bonds of alkanes at room temperature with the rate comparable to that of the Cytochrome P-450 enzyme. ¹⁰
2.	Fe-Phthalocyanine in zeolite X and Y	Oxidation of alkanes by iodobenzene with improved yield and altered selectivity as compared to the 'free' or unencapsulated complex. ⁴⁹
3.	Fe-Phthalocyanine in zeolite Y and VPI-5	Selective oxyfunctionalization of alkanes using <i>tert</i> -butyl hydroperoxide with higher activity than that of the 'free' complex. ⁵⁰

4.	Fe-phthalocyanine in zeolites	oxidation of 1-octene to 2-octanone and in the allylic oxidation of cyclohexene to 3-acetoxycyclohexene. ⁵¹
5.	Fe and Co phthalocyanines in zeolite Y	Oxidation of cis-pinane. ⁵²
6.	Phthalocyanines and substituted (chloro- and nitro-) phthalocyanines of copper, cobalt and iron encapsulated in zeolites X and Y	Oxidation of cyclohexane to cyclohexanol, cyclohexanone and adipic acid. ⁵³
7.	Fe phthalocyanine (FePc) and Co phthalocyanine (as free complexes as well as encapsulated in zeolite-Y	Mild, aerobic oxidation of hydroquinone. A remarkable rate enhancement was observed with the encapsulated catalysts. ⁵⁴
8.	Fe-Tetra Methyl Porphyrin (TMP) and MnTMP in zeolite Y	Oxidation of cyclohexane to cyclohexanol and cyclohexanone with improved yield. ⁵⁵
9.	Metal phthalocyanine complexes (MPc; M=V, Co and Cu) are encapsulated in zeolite-Y	Enhanced phenol hydroxylation activity with H ₂ O ₂ compared to the “neat” complexes in homogeneous medium. ⁵⁶
10.	Mn-tetrakis (N, N, N)-trimethylanilinium) porphyrin in zeolite-Y	Catalytic epoxidation of cyclohexene with <i>tert</i> -butyl hydroperoxide with high activity and selectivity. ⁵⁷
11.	<i>meso</i> -Tetrakis (5-trimethylammonioethyl)porphyrin (TMAP) was incorporated in MCM-41	Catalytic activity of the copper porphyrins was evaluated in the oxidative bleaching reaction of the azo dye β-naphthol violet. ⁵⁸

Table 1.2: Catalytic activity of zeolite encapsulated metal-bipyridyl and amino acids complexes.

S.No	Encapsulated complex	Reaction/ Reference
1.	Ru-tris(bipydyl) [Ru(bpy) ₃] ³⁺ complex in zeolite-Y	Slow but efficient oxidation of water to dioxygen. ⁵⁹
2.	<i>cis</i> -[Mn(bpy) ₂] ²⁺ in zeolite-X and Y	Selective epoxidation of alkenes without complications from competing processes such as self-oxidation. ⁶⁰
3.	{(bpy) ₂ Ru ⁴⁺ =O} ²⁺ in zeolite-Y	Oxidation of PPh ₃ and hydrocarbons. ⁶¹
4.	Mixed ligand complexes of 2,2'-bipyridine and 1,10-phenanthroline with iron(III) and nickel(II) have been encapsulated into a zeolite Y	Catalytically active toward the oxidation of 2-phenyl phenol (OPP). ⁶²
5.	Cu(Histidine) complex in zeolite-Y	Olefin epoxidation and alcohol oxidation at relatively low temperature in presence of peroxide. ⁶³
6.	Fe-proline, Fe-histidine and Cu-valine in zeolite X	Oxidation of cyclohexane and benzylic alcohols. ⁶⁴

Table 1.3: Catalytic activity of zeolite encapsulated metal-salen complexes.

S.No	Encapsulated Complex	Reaction/ Reference
1.	Co(II)(salen) in Zeolite-Y	Conversion of benzyl chloride to phenylacetic acid. ⁶⁵
2.	Cu(II) (salen) and Mn(III) (salen) in zeolite X and Y	Decomposition of H ₂ O ₂ and tert-butyl hydroperoxide; low-temperature oxidation of phenol, styrene and p-xylene with enhanced rate. ⁶⁶
3.	Mn(III) (salen) in zeolite EMT	Formation of high enantiomeric excess in the epoxidation of aromatic alkenes with NaOCl. ⁶⁷

4.	Mn(salen) ⁺ in zeolite-Y	Slow but selective oxidation of olefins based on olefin size and ability to diffuse through the zeolite cages. ⁶⁸
5.	Pd(salen) in zeolite X and Y	Selective hydrogenation of hex-1-ene over cyclohexene at 25°C. ⁶⁹
6.	Cr(III), Fe(III), Bi(III), Ni(II), and Zn(II) complexes of <i>N,N'</i> -bis(salicylidene)propane-1,3-diamine (H ₂ salpn) encapsulated in NaY zeolite	Fe(salpn)-NaY catalyst exhibited the highest carvacrol conversion. ⁷⁰
7.	Oxovanadium(IV), copper(II) and nickel(II) complexes of Schiff base in zeolite Y	Oxidation of styrene, cyclohexane and methyl phenyl sulfide ⁷¹ .
8.	Co-Schiff base complexes in zeolite Y	Zeolite-encapsulated Co complexes were found to be more active and stable than the neat Co complexes. Zeolite-encapsulated Co salophen shows the highest activity; and the conversion of methanol and selectivity to DMC was 25.4 and 99.5%, respectively. ⁷²
9.	(M = Cu, Co, Fe and Mn) tetrahydro-Schiff base complexes in zeolite Y	Cu-[H ₄]salen/Y, are highly active for the oxidation of cycloalkanes. ¹⁴
10.	Transition metal (M = Mn(II), Co(II), Ni(II) and Cu(II)) complexes with tetrahydro-salophen in zeolite Y.	Oxidation of cyclohexane with zeolite encapsulated complexes with better reactivity. ⁷³
11.	Fe-Schiff-base complexes encapsulated in various alkali metal cation exchanged zeolite-Y.	Catalytically active toward the oxidative coupling of 2-naphthol. ³⁶

12.	Nickel(II) and copper(II) complexes of the Schiff base ligand <i>O,O'</i> -trimethyl bis (salicylidene isonicotinyldihydrazone) in zeolite Y	Copper(II) [Cu(II)L·2ClO ₄ , Cu(II)L–Y] complexes showed better activity than the nickel(II) complexes [Ni(II)L·2ClO ₄ , Ni(II)L–Y] in both BH and RhB degradation reactions. ⁷⁴
13.	Chiral Schiff-base complexes of copper(II) encapsulated inside the cavity of zeolite-NaY	Zeolite-encapsulated chiral copper(II) Schiff-base complexes are found to give a high-enantioselective and has shown higher catalytic efficiency than their homogeneous counterparts under identical conditions. ¹⁹
14.	Oxido-vanadium Schiff base complexes in zeolite Y	Zeolite Y encapsulated complexes were found to show better catalytic activity than the mononuclear homogeneous catalyst but less than the dinuclear species. ⁷⁵
15.	Chiral Ni(II)-Schiff base complexes synthesized inside the cavity of zeolite-Y	High catalytic transformation of aldehydes with nitro-methane to nitro-aldol product (92% yield and 83% ee, <i>S</i> -isomer) was achieved at 10 °C. ⁷⁶

1.3. Characterization of zeolite encapsulated complexes

There is wide range of reports available in literature which deals with the modified catalytic activities of zeolite encapsulated metal complexes. While comparatively less number of reports are available which deal with the adopted geometry and detailed characterization of the encapsulated complex within the host zeolite lattice. It is already a well-established fact that encapsulation certainly leads alteration in the geometry of the ‘guest complex’ from its ‘free state’. These small changes in the structure of the complex could be a motive of modified functionality of the system. One of the earliest reports by Mizuno and Lunsford

shows that the spin-state of encapsulated Co(II)tris(bipyridyl) in zeolite-Y is quite different from that of this complex ion either in solution or in the solid state. Interestingly, the cobalt complex in the encapsulated state undergoes a thermally driven spin-conversion from the low-spin to high-spin state with temperature.⁴¹ A detailed spectroscopic and magnetic studies of this system was reported by Tiwary and Vasudevan.²¹ The magnetic moment of the un-encapsulated Co(II)tris(bipyridyl) complex ion remains constant at $\sim 4.6 \mu_B$ ($S = 3/2$) over a wide temperature range, while the complex in encapsulated state shows a regular increase from $1.9 \mu_B$ ($S = 1/2$) at low temperature to a value intermediate between the high spin (HS) ($S = 3/2$) and low spin (LS) ($S = 1/2$) values at higher temperatures (Figure 1.5). The optical reflectance spectrum of the encapsulated complex also indicates the features arising from transitions due to both from the high-spin as well as low-spin ground states of a Co^{2+} ion. Modeling, Magnetic and spectroscopic studies of the $[\text{Co}(\text{bpy})_3]^{2+}$ complex reveal that it adopts comparatively less distorted octahedral geometry under encapsulation with respect to its “free” state.²¹

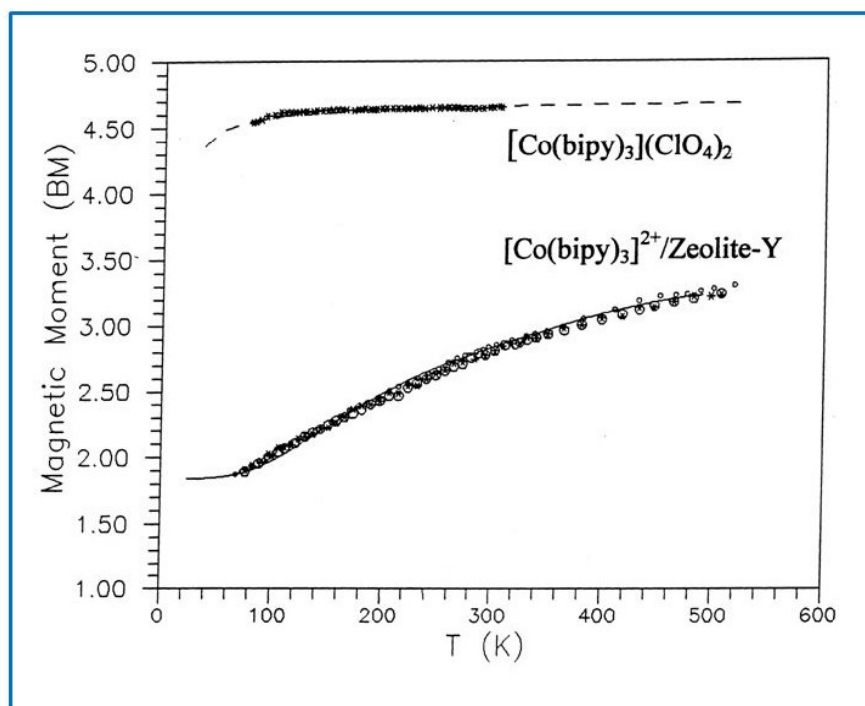


Figure 1.5: Magnetic moments of (a) $[\text{Co}(\text{bpy})_3](\text{ClO}_4)_2$ and (b) $[\text{Co}(\text{bpy})_3]^{2+}$ encapsulated in zeolite Y.²¹ (Adapted from ref. 21)

Another earliest report has explored the remarkable effects on the magnetic properties and oxygen binding behavior of the cobalt salen complex after encapsulation in zeolite Y.³⁵ Author has reported the remarkable stability of this hybrid systems towards the irreversible oxygen binding which in turn reinforces the existing analogies between zeolite-encapsulated active sites and natural enzyme systems.³⁵ A detailed study of the Co phthalocyanine complex “free” and encapsulated in zeolite-Y and MCM-41 has been carried out by Ray and Vasudevan.²² The authors have studied the effect of the size and topology of the host supercage on the adopted geometry of the encapsulated complex (Given in Figure 1.6). The electronic spectrum of CoPc encapsulated in zeolite-Y complex shows that the splitting in phthalocyanine Q band is surely signature of a lowering of symmetry of complex. In support of this fact, vibrational spectroscopic studies have suggested a breakdown of the mutual exclusion principle; IR modes of encapsulated CoPc complex become Raman active and vice-versa. This loss of center of inversion is a consequence of the non planar geometry that the complex required to adopt on encapsulation inside the 12.7 Å diameter supercage of zeolite-Y.

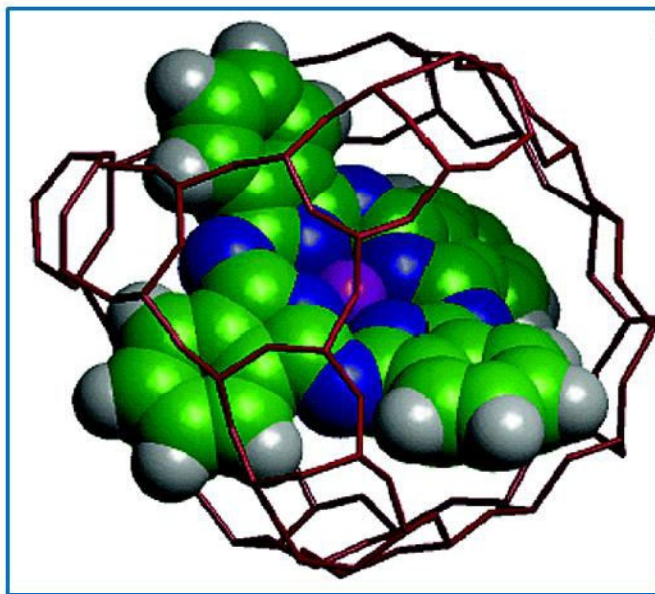


Figure 1.6: Molecular graphics representation of a square-planar Co phthalocyanine molecule encapsulated within the supercage of zeolite-Y.²² (Adapted from ref. 22)

In addition to that, the report have confirmed that CoPc complex experienced saddle-type distortion after encapsulation in zeolite Y and as its consequences, the magnetic moment of

encapsulated complex is enhanced from its value in the unencapsulated or free state. This altered magnetic behavior is surely related to the extent of distortion of the CoPc from planar geometry since the same complex when encapsulated in the MCM-41 (comparatively larger voids), maintains parallel magnetic behavior to its free state (Figure 1.7). The authors have concluded that lowering of the energy difference between the low-spin and high-spin states is a consequence of the distortion from planar geometry of the encapsulated CoPc.²²

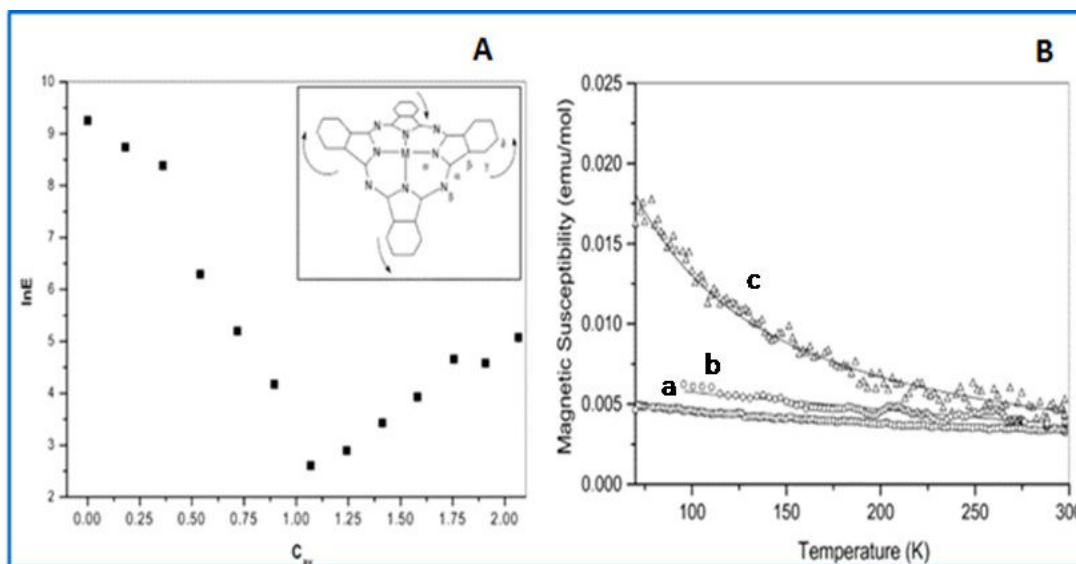


Figure 1.7: (A) Total potential energy for CoPc encapsulated in zeolite-Y as a function of the average rms displacement of the atoms of the Pc ring from planar geometry (C_{av}). The saddle-type distortion is shown in the inset. (B) Temperature variation of magnetic susceptibilities of (a) CoPc in free state (b) encapsulated in MCM-41 and in (c) zeolite Y. ²² (Adapted from ref. 22)

In another report by Ganesan and Viswanathan,⁷⁷ the authors have indicated that when encapsulated in different zeolites (NaY, KL, AIMCM-41, Na β , and Na-ZSM-5) the Bis(ethylenediamine)copper(II) $[\text{Cu}(\text{NH}_2\text{CH}_2\text{CH}_2\text{NH}_2)_2]^{2+}$ complex shows different geometries from its free state. Using optical absorption data from several sources of copper complexes, it is assumed that the d-d band at 18315 cm^{-1} corresponding to the ${}^2\text{B}_{1g} \rightarrow {}^2\text{B}_{2g}$ transition is blue-shifted on encapsulation in NaY zeolite and red-shifted in Na β zeolite, Na-ZSM-5 zeolite and AIMCM-41.

With the help of DFT studies, authors have justified that the change of redox potential of the encaged complexes are due to the shuffling of energy level and a change in the positions of the highest occupied molecular orbital (HOMO) and lowest unoccupied molecular orbital

(LUMO) levels of the metal with the help of DFT studies, authors have justified that the change of redox potential of the encaged complexes are due to the shuffling of energy level and a change in the positions of the highest occupied molecular orbital (HOMO) and lowest unoccupied molecular orbital (LUMO) levels of the metal complexes.⁷⁷

The electroactivity of zeolite-encapsulated redox-active transition metal complexes, $\{M(L)\}Z$, was explored for Co(salen) and $[Fe(bpy)_3]^{2+}$ formed in NaY zeolite.⁷⁸ It was observed that both the complexes support an extrazeolite redox mechanism involving an external surface topological isomer that is faradaically durable for hours in the absence of lattice damage.⁷⁸ Intermolecular structural and dynamic effects in Ru(II) tris(bipyridyl) $[Ru(bpy)_3]^{2+}$ complex ion entrapped in zeolite-Y have been discussed by Dutta and co-workers.⁷⁹ Major spectral perturbation including a red shift of the metal-to-ligand charge-transfer band, shifts in bipyridine ring breathing modes and quenching of emission lifetime are observed. The results are interpreted to suggest that the structure of the encapsulated $[Ru(bpy)_3]^{2+}$ at low loading levels resembles that of the complex ion in solution. At higher loading levels, molecules occupy neighboring supercages and interact with one another through the 7 Å ring openings. It is claimed that the driving force behind the $[Ru(bpy)_3]^{2+}$ --- $[Ru(bpy)_3]^{2+}$ aggregation effects, is due to the highly polar nature of the intracrystalline space.⁷⁹

Umemura *et. al* have investigated the interesting effect of structural change due to the interaction between the encapsulated 6-coordinated Fe(II) complexes and the zeolite lattice. Encapsulation of Fe(II) complex ions, $[FeL_3]^{2+}$, within the supercage of zeolite-Y. The authors have explored the mössbauer and optical spectroscopic studies of complexes with a series of ligands with different bulk and have revealed that the complexes ($[Fe(bpy)_3]^{2+}$ and $[Fe(phen)_3]^{2+}$) of a comparable size to that of the zeolite cavity undergo trigonal prismatic distortion from octahedral geometry on encapsulation, whereas smaller complexes ($[Fe(en)_3]^{2+}$ and $[Fe(amp)_3]^{2+}$) does not show any such distortion and remains undistorted. However larger complexes $[Fe(dmbpy)_3]^{2+}$ and $[Fe(dmphen)_3]^{2+}$ with the molecular dimension larger than that of the zeolite cavity cannot even be encapsulated in zeolite Y. Each of the complex ion $[Fe(bpy)_3]^{2+}$ and $[Fe(phen)_3]^{2+}$, is located in the supercage with its 3-fold axis parallel to that of the supercage; each of the three ligands face to the 12-membered

ring of the supercage. The complexes are reported to be twisted around their 3-fold axes from an octahedron to a trigonal prism (Figure 1.8).

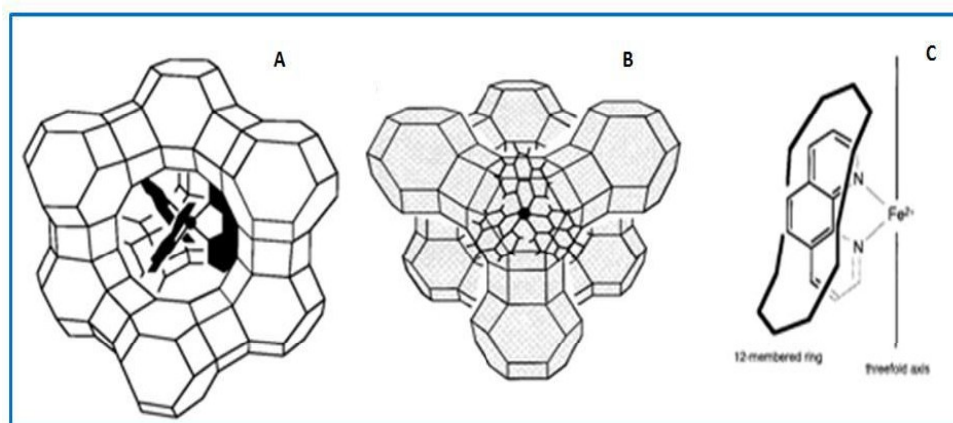


Figure 1.8: Schematic views of (A and B) $[\text{Fe}(\text{phen})_3]^{2+}$ in the supercage and (C) one of the three ligands facing the 12-membered ring of the cage.⁸⁰ (Adapted from ref. 80)

In another report the spectroscopic and photophysical properties of zeolite-Y-encaged $[\text{Ru}(\text{bpy})_3]^{2+}$ co-doped with either $[\text{Fe}(\text{bpy})_3]^{2+}$ or $[\text{Fe}(\text{tpy})_2]^{2+}$ over a range of iron complex loadings are presented.⁸¹ The zeolite encaged iron complexes are found to quench both intensity and lifetime of the $[\text{Ru}(\text{bpy})_3]^{2+}$ complex, $[\text{Fe}(\text{bpy})_3]^{2+}$ has dynamically quenched $[\text{Ru}(\text{bpy})_3]^{2+}$ through nonradiative energy transfer whereas $[\text{Fe}(\text{tpy})_2]^{2+}$ appears to quench only through a radiative or trivial energy transfer mechanism.

M. Jafarian *et al.* have explored the fact that when Ni(II) -(N,N-bis(2,4-dihydroxyacetophenone)- 2,2-dimethylpropandiimine $[\text{Ni}^{2+}\{\text{salnptn}(4\text{-OH})_2\}]$ complex encapsulated within the supercage of Na-zeolite-Y, the complex undergoes distortion under the influence of constraint imposed by zeolite framework (Figure 1.9). The authors have observed the peak broadening in cyclic voltammograms upon encapsulation of which has been correlated with the change in the positions of the HOMO and LUMO levels of the molecular systems. Simultaneously the electrochemical studies exhibit the oxidation of alcohols on the $\text{Ni}^{\text{II}}\{\text{salnptn}(4\text{-OH})_2\}\text{-Y/CPE}$ is catalyzed through the mediated electron transfer, whereas for the poly- $\text{Ni}^{\text{II}}\{\text{salnptn}(4\text{-OH})_2\}$ film, Ni^{III} sites act as active surface for the direct electro-oxidation of alcohols.²³ R.C. Deka and coworkers have identified the structural changes in adopted geometry of the complex after encapsulation in zeolite Y experimentally as well as theoretically.^{20, 36, 82}

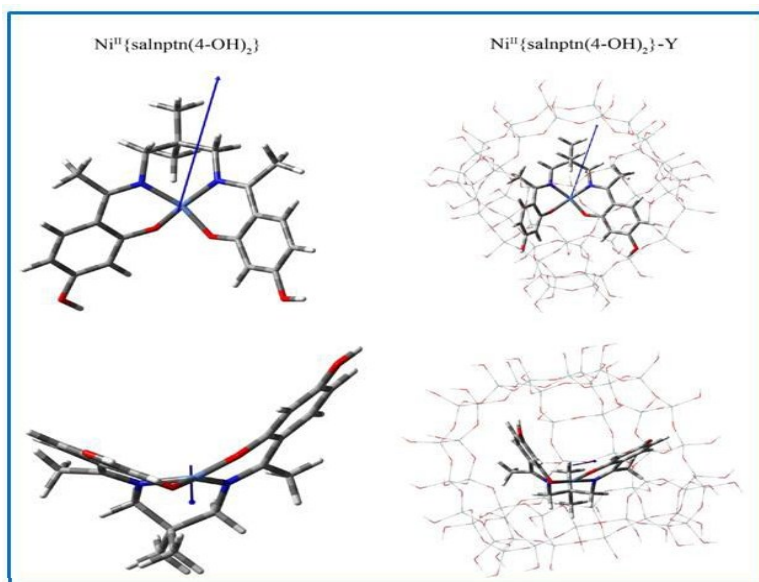


Figure 1.9: Different perspective of DFT optimized structure of (left) the free and (right) the encapsulated nickel Schiff-base complex obtained at the B3LYP level.²³ (Adapted from ref. 23)

With the help of spectrochemical study and the DFT calculations authors have concluded that when encapsulated within the supercage of zeolite Y bis(1,10-phenanthroline) cobalt(II) complex, undergoes distortion under the influence of a constrained zeolite framework. As a consequence, encapsulated Co-phenanthroline complex has exhibited peak broadening in cyclic voltammetry (Given in Figure 1.10) and it is surely a reason for the change observed in the positions of the HOMO and LUMO levels of the molecular systems.⁸²

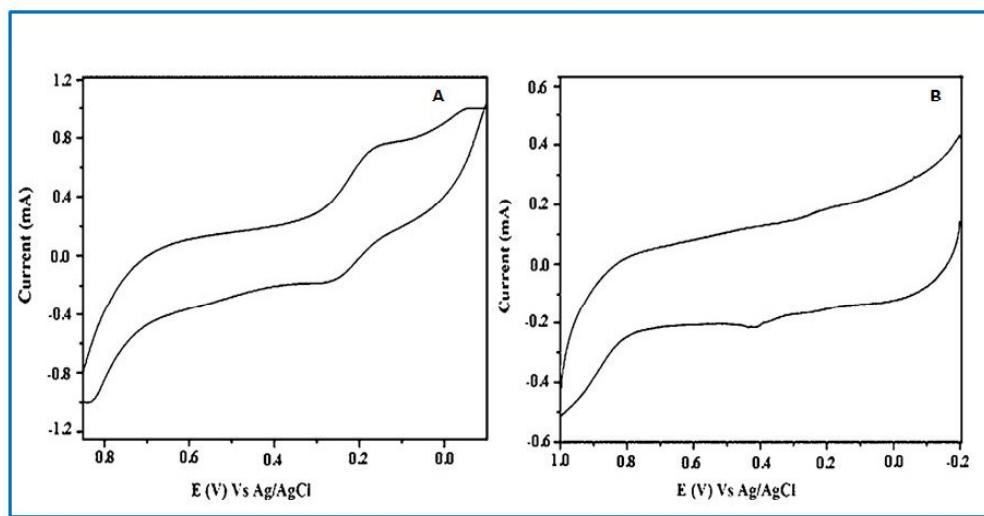


Figure 1.10: Cyclic voltammogram of (A) CoPhen (neat) and (B) CoPhenY.⁸² (Adapted from ref 82)

The authors have extended the study and have synthesized zeolite Y encapsulated tris(1,10-phenanthroline) complexes of iron(II), copper(II), and zinc(II) ions. Interestingly, it is observed that the Fe-phenanthroline and Cu-phenanthroline complexes are formed inside the zeolite supercage,²⁰ whereas the corresponding zinc complex is tethered via the formation of H-bond on the external surface of zeolite Y.

Comparative XRD patterns of encapsulated complexes are found essentially similar with XRD patterns of pure and metal exchanged zeolites, though intensity reversal in the relative peaks at $2\theta = 10$ and 12° for the 220 and 311 reflections for the Fe-phenanthroline and Cu-phenanthroline complexes have appeared which is an empirically established fact for the successful signature of the encapsulation process.²⁰ But encapsulated Zn-phenanthroline complex has not shown such intensity reversal in XRD patterns since it is tethered on surface of the host. However the results of the spectrochemical and DFT studies show that encapsulation or tethering of the metal complexes leads to the red shift of the MLCT and intra-ligand transitions and lifting of the HOMO and LUMO levels under the influence of the Coulombic electrostatic field and the space restraints imposed by the zeolite mantle.²⁰ Authors further have studied the iron (III)-Schiff-base complexes (where ligands = *N,N'*-bis(salicylidene)ethylenediamine and *N,N'*-disalicylidene-1,2-phenylenediamine) encapsulated within various alkali exchanged zeolites.³⁶

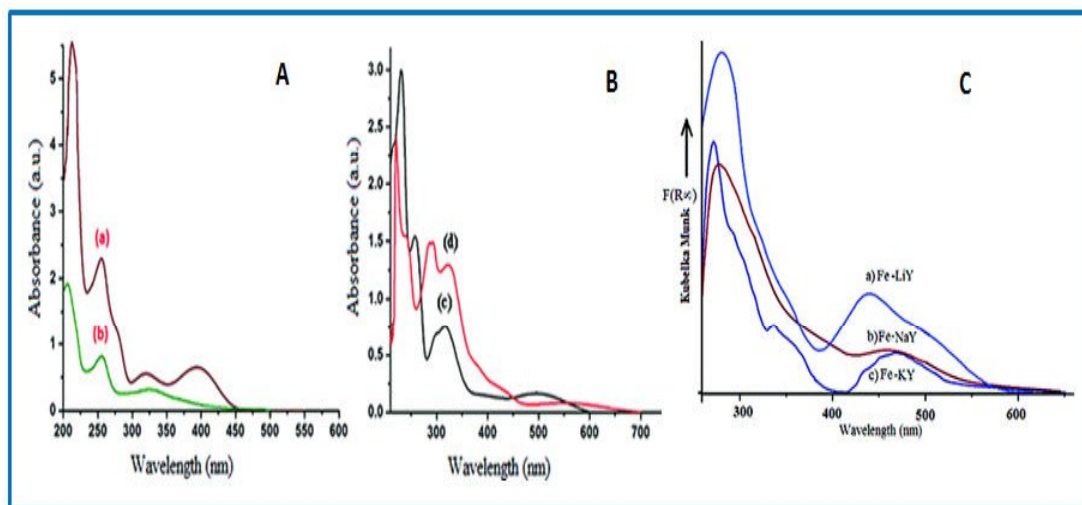


Figure 1.11: (A-B) UV-Vis spectra of (a) *N,N*-bis(salicylidene)ethylenediamine (Salen), (b) *N,N'*-disalicylidene-1,2-phenylenediamine (Salophen), (c) neat Fe-Salen complex, and (d)

neat Fe-Salophen complex And (C) DR spectra of ion exchanged zeolites (a) Fe-LiY, (b) Fe-NaY, (c) Fe-KY.³⁶ (Adapted from ref. 36)

The influence of alkali metal cations (Li^+ , K^+ and Na^+) on the optical, redox, and catalytic properties of the encapsulated Fe(III) Schiff-base complexes have been studied and is observed that the size of the exchangeable counter cation has profound influence on the LMCT transitions and the average reduction potential of the encapsulated iron complexes, since larger alkali cation starting from Li^+ to K^+ considerably have shown red-shift in the lower and the higher energy electronic bands (Shown in Figure 1.11).³⁶

Kandasamy Jothivenkatachalam and coworkers have studied encapsulated 5,7,7,12,14,14-hexamethyl-1,4,8,11-tetraazacyclotetradecane [tet-a] Nickel(II) in zeolite Y.⁸³ The observed blue shift in d-d region of optical spectra of the encapsulated complex and the DFT and TD-DFT studies of the complex in the both states have provided further evidence about distortion in the geometry of the complex. Calculated chemical hardness has suggested the additional stability of encapsulated complex compared to its free form. The report has concluded that constrained environment and steric factor of the host zeolite Y have intense impact on the geometry of the complex since the complex is effective photo catalyst in the encapsulated state.⁸³ Recently, Balachandran Unni Nair and coworkers have studied the synthesis of mixed ligand complexes of 2,2-bipyridine and 1,10-phenanthroline with iron(III) and nickel(II) in a zeolite Y (Given in Figure 1.14).⁶²

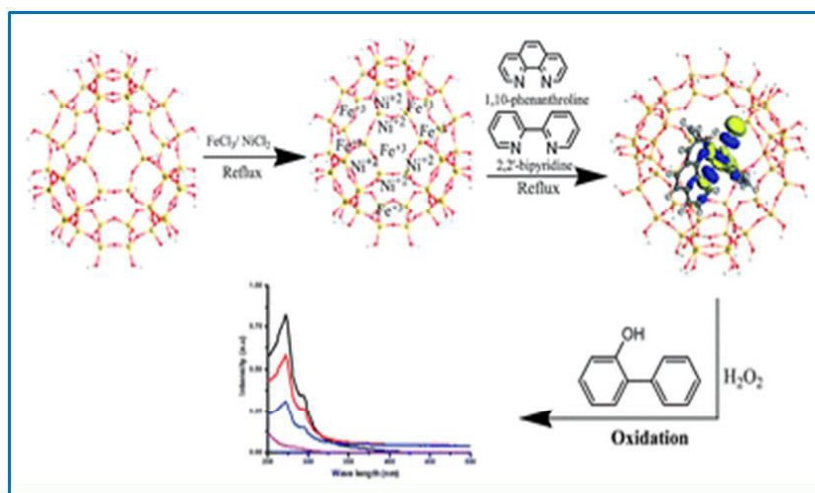


Figure 1.12: 2,2-bipyridine and 1,10-phenanthroline with iron(III) and nickel(II) in a zeolite Y.⁶² (Adapted from ref 62)

The different techniques have suggested that the change in HOMO–LUMO energies, global hardness, softness value, and change in bond angle, dihedral angle and modified enhanced reactivity of the metal complexes upon encapsulation is surely a sign of the deformation in the geometry of the complex after encapsulation in zeolite Y.⁶²

In the present thesis, the objective is to study the effect of size and topology of the zeolite-Y supercage on the structure of encapsulated square-planar complexes also to explore the relationship existing between modified geometry or altered functionality of the encapsulated complex. Encapsulated metal-salen complexes are synthesized by the *flexible ligand* method. Both absorption, vibrational and XPS studies provide evidence for the formation of the complex within the supercage of zeolite-Y. Spectroscopic and magnetic studies indicate a significant deviation in the geometry adopted by the encapsulated complex while comparing it with that in the unencapsulated state.

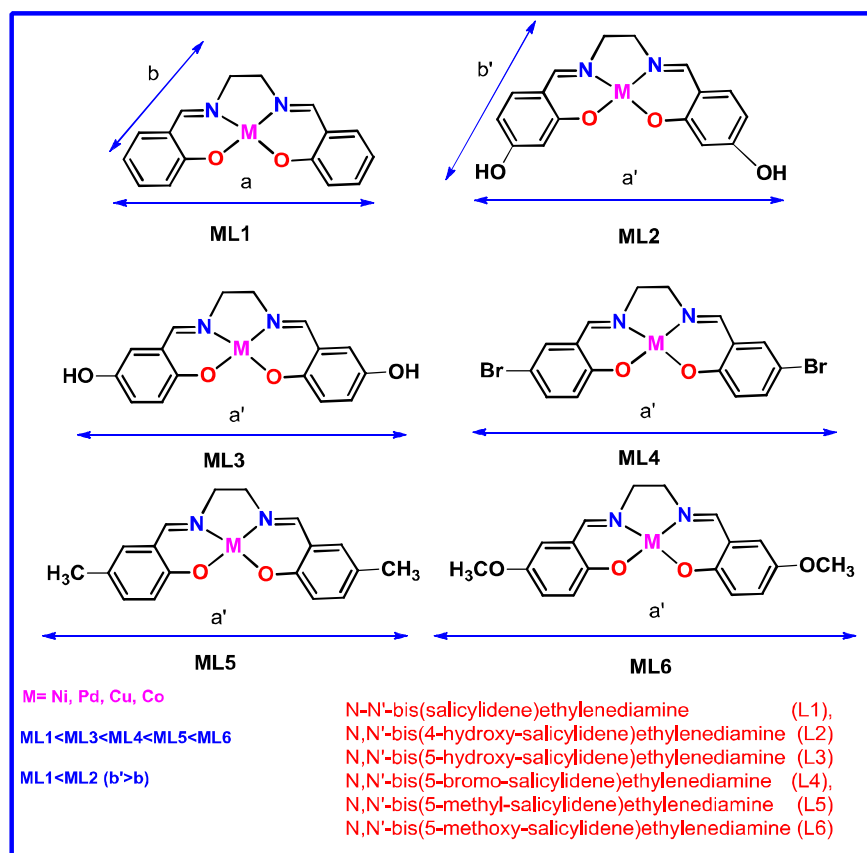


Figure 1.13: Schematic representation with the molecular dimension (end-to-end distance) of M(salen) complexes. (where M = Ni, Pd, Co, Cu)

These synthesized encapsulated complexes are employed as catalysts on different systems like oxidation of styrene, thioanisole and degradation of rhodamine B. The electronic effect of the different substituent groups present in the catalyst play the decisive role towards their reactivity in the homogeneous phase but after the encapsulation in zeolite Y, reactivity is mainly governed by the extent of steric hindrance imposed by host topology on the guest complexes which probably in an way, plays an important role in tuning the the electronic properties towards a particular catalytic reaction. This is also supported by DFT studies and the results are not surprising since the molecular dimension of the M(II) (salen) complexes are comparable or progressively larger than that of the void of zeolite-Y

REFERENCES

1. P. B. Venuto, *Microporous Mater.*, 1994, **2**, 297-411.
2. P. B. Venuto, in *Stud. Surf. Sci. Catal*, eds. S.-K. I. Hakze Chon and U. Young Sun, Elsevier, 1997, vol. Volume 105, pp. 811-852.
3. D. E. De Vos, B. F. Sels and P. A. Jacobs, *CATTECH*, 2002, **6**, 14-29.
4. K. J. Balkus and A. G. Gabrielov, *J. Inclusion Phenom. Mol. Recognit. Chem.*, 1995, **21**, 159-184.
5. N. Herron, G. D. Stucky and C. A. Tolman, *Inorg. Chim. Acta*, 1985, **100**, 135-140.
6. N. Herron, *Inorg. Chem*, 1986, **25**, 4714-4717.
7. N. Herron, *J Coord Chem.*, 1988, **19**, 25-38.
8. S. Deshpande, D. Srinivas and P. Ratnasamy, *J. Catal.*, 1999, **188**, 261-269.
9. K. Mori and H. Yamashita, *Chem. Eur. J.*, 2016, **22**, 11122-11137.
10. R. F. Parton, I. F. J. Vankelecom, M. J. A. Casselman, C. P. Bezoukhanova, J. B. Uytterhoeven and P. A. Jacobs, *Nature*, 1994, **370**, 541-544.
11. D. Srinivas and S. Sivasanker, *Catal. Surv. Asia*, 2003, **7**, 121-132.
12. C. R. Jacob, S. P. Varkey and P. Ratnasamy, *Microporous Mesoporous Mater.*, 1998, **22**, 465-474.
13. R. F. Parton, L. Uytterhoeven and P. A. Jacobs, in *Stud. Surf. Sci. Catal*, eds. J. B. C. B. D. D. G. P. R. M. M. Guisnet and C. Montassier, Elsevier, 1991, vol. Volume 59, pp. 395-403.

14. C. Jin, W. Fan, Y. Jia, B. Fan, J. Ma and R. Li, *J. Mol. Catal. A: Chem.*, 2006, **249**, 23-30.
15. J. Poltowicz, K. Pamin, E. Tabor, J. Haber, A. Adamski and Z. Sojka, *Appl. Catal., A*, 2006, **299**, 235-242.
16. M. Silva, C. Freire, B. de Castro and J. L. Figueiredo, *J. Mol. Catal. A: Chem.*, 2006, **258**, 327-333.
17. K. O. Xavier, J. Chacko and K. K. Mohammed Yusuff, *Appl. Catal., A*, 2004, **258**, 251-259.
18. M. R. Maurya, S. J. J. Titinchi, S. Chand and I. M. Mishra, *J. Mol. Catal. A: Chem.*, 2002, **180**, 201-209.
19. K. K. Bania, G. V. Karunakar, K. Goutham and R. C. Deka, *Inorg. Chem.*, 2013, **52**, 8017-8029.
20. K. K. Bania and R. C. Deka, *J. Phys. Chem. C*, 2012, **116**, 14295-14310.
21. S. K. Tiwary and S. Vasudevan, *Inorg. Chem.*, 1998, **37**, 5239-5246.
22. S. Ray and S. Vasudevan, *Inorg. Chem.*, 2003, **42**, 1711-1719.
23. M. Jafarian, M. Rashvand avei, M. Khakali, F. Gobal, S. Rayati and M. G. Mahjani, *J. Phys. Chem. C*, 2012, **116**, 18518-18532.
24. F. Bedioui, *Coord. Chem. Rev.*, 1995, **144**, 39-68.
25. Y. Ma, W. Tong, H. Zhou and S. L. Suib, *Microporous Mesoporous Mater.*, 2000, **37**, 243-252.
26. K. D. Hammonds, V. Heine and M. T. Dove, *J. Phys. Chem. B*, 1998, **102**, 1759-1767.
27. L. V. Rees, *Journal*, 1992.
28. R. G. Bell, R. A. Jackson and C. R. A. Catlow, *Zeolites*, 1992, **12**, 870-871.
29. C.-S. Yang, J. M. Mora-Fonz and C. R. A. Catlow, *J. Phys. Chem. C*, 2011, **115**, 24102-24114.
30. A. Corma, *Chem. Rev.*, 1995, **95**, 559-614.
31. J. Hagen, in *Industrial Catalysis*, Wiley-VCH Verlag GmbH & Co. KGaA, 2015, DOI: 10.1002/9783527684625.ch5, pp. 99-210.
32. C.-n. Wu and K.-j. Chao, *J. Chem. Soc., Faraday Trans.*, 1995, **91**, 167-173.
33. J. Weitkamp, *Solid State Ion.*, 2000, **131**, 175-188.
34. N. Herron, *J Coord Chem.*, 1988, **19**, 25-38.

35. N. Herron, *Inorg. Chem.*, 1986, **25**, 4714-4717.
36. K. K. Bania, D. Bharali, B. Viswanathan and R. C. Deka, *Inorg. Chem.*, 2012, **51**, 1657-1674.
37. R. J. Correa, G. C. Salomao, M. H. N. Olsen, L. Cardozo Filho, V. Drago, C. Fernandes and O. A. C. Antunes, *Appl. Catal., A*, 2008, **336**, 35-39.
38. M. Maurya, S. Titinchi, S. Chand and I. Mishra, *J. Mol. Catal. A: Chem.*, 2002, **180**, 201-209.
39. M. R. Maurya, A. K. Chandrakar and S. Chand, *J. Mol. Catal. A: Chem.*, 2007, **270**, 225-235.
40. S. Ernst and O. Batreau, *Stud. Surf. Sci. Catal.*, 1995, **94**, 479-486.
41. K. Mizuno and J. H. Lunsford, *Inorg. Chem.*, 1983, **22**, 3484-3486.
42. K. J. Balkus and J. P. Ferraris, *J. Phys. Chem.*, 1990, **94**, 8019-8020.
43. E. Paez-Mozo, N. Gabriunas, F. Lucaccioni, D. D. Acosta, P. Patrono, A. La Ginestra, P. Ruiz and B. Delmon, *J. Phys. Chem.*, 1993, **97**, 12819-12827.
44. J. P. Ferraris, K. J. Balkus and A. Schade, *J. Inclusion Phenom. Mol. Recognit. Chem.*, 1992, **14**, 163-169.
45. F. Bedioui, L. Roue, L. Gaillon, J. Devynck, S. L. Bell and K. J. Balkus, Jr., *Prepr. - Am. Chem. Soc., Div. Pet. Chem.*, 1993, **38**, 529-535.
46. K. J. Balkus, Jr., A. A. Welch and B. E. Gnade, *J. Inclusion Phenom. Mol. Recognit. Chem.*, 1991, **10**, 141-151.
47. K. J. Balkus, A. G. Gabrielov, S. L. Bell, F. Bedioui, L. Roue and J. Devynck, *Inorg. Chem.*, 1994, **33**, 67-72.
48. K. J. Balkus, C. D. Hargis and S. Kowalak, in *Supramolecular Architecture*, American Chemical Society, 1992, vol. 499, ch. 24, pp. 347-354.
49. N. Herron, G. D. Stucky and C. A. Tolman, *J. Chem. Soc., Chem. Commun.*, 1986, DOI: 10.1039/C39860001521, 1521-1522.
50. M. Guisnet, C. International Symposium on Heterogeneous and C. Fine, Heterogeneous catalysis and fine chemicals II : proceedings of the 2nd international symposium, Poitiers, October 2-5, 1990, <http://site.ebrary.com/id/10258726>).
51. Á. Zsigmond, F. Notheisz, Z. Szegetes and J. E. Bäckvall, in *Stud. Surf. Sci. Catal*, eds. H. G. K. I. K. H.K. Beyer and J. B. Nagy, Elsevier, 1995, vol. Volume 94, pp. 728-735.

52. A. A. Valente and J. Vital, in *Stud. Surf. Sci. Catal*, eds. A. B. H.U. Blaser and R. Prins, Elsevier, 1997, vol. Volume 108, pp. 461-468.
53. R. Raja and P. Ratnasamy, *Catal. Lett.*, 1997, **48**, 1-10.
54. Á. Zsigmond, F. Notheisz and J.-E. Bäckvall, *Catal. Lett.*, 2000, **65**, 135-139.
55. M. Nakamura, T. Tatsumi and H.-o. Tominaga, *Bull. Chem. Soc. Jpn.*, 1990, **63**, 3334-3336.
56. S. Seelan and A. K. Sinha, *Appl. Catal., A*, 2003, **238**, 201-209.
57. B.-Z. Zhan and X.-Y. Li, *Chem. Commun.*, 1998, DOI: 10.1039/A706030K, 349-350.
58. B. T. Holland, C. Walkup and A. Stein, *J. Phys. Chem. B*, 1998, **102**, 4301-4309.
59. M. Ledney and P. K. Dutta, *J. Am. Chem. Soc.*, 1995, **117**, 7687-7695.
60. P.-P. Knops-Gerrits, D. De Vos, F. Thibault-Starzyk and P. A. Jacobs, *Nature*, 1994, **369**, 543-546.
61. P. K. Dutta and S. K. Das, *J. Am. Chem. Soc.*, 1997, **119**, 4311-4312.
62. S. L. Hailu, B. U. Nair, M. Redi-Abshiro, R. Aravindhan, I. Diaz and M. Tessema, *RSC Adv.*, 2015, **5**, 88636-88645.
63. B. M. Weckhuysen, A. A. Verberckmoes, I. P. Vannijvel, J. A. Pelgrims, P. L. Buskens, P. A. Jacobs and R. A. Schoonheydt, *Angew. Chem. Int. Ed. (English)*, 1996, **34**, 2652-2654.
64. J. Dzierzak, M. Lefenfeld and R. Raja, *Top. Catal.*, 2009, **52**, 1669-1676.
65. C. A. Bessel and D. R. Rolison, *J. Am. Chem. Soc.*, 1997, **119**, 12673-12674.
66. C. R. Jacob, S. P. Varkey and P. Ratnasamy, *Microporous Mesoporous Mater.*, 1998, **22**, 465-474.
67. C. Bowers and P. K. Dutta, *J. Catal.*, 1990, **122**, 271-279.
68. S. B. Ogunwumi and T. Bein, *Chem. Commun.*, 1997, DOI: 10.1039/A607879F, 901-902.
69. S. Kowalak, R. C. Weiss and K. J. Balkus, *J. Chem. Soc., Chem. Commun.*, 1991, DOI: 10.1039/C39910000057, 57-58.
70. A. Güneş, O. Bayraktar and S. Yılmaz, *Ind. Eng. Chem. Res.*, 2006, **45**, 54-61.
71. M. R. Maurya, A. K. Chandrakar and S. Chand, *J. Mol. Catal. A: Chem.*, 2007, **274**, 192-201.
72. D. Zhu, F. Mei, L. Chen, T. Li, W. Mo and G. Li, *Energy Fuels*, 2009, **23**, 2359-2363.

73. M. Salavati-Niasari, M. Shakouri-Arani and F. Davar, *Microporous Mesoporous Mater.*, 2008, **116**, 77-85.
74. G. Ramanjaneya Reddy, S. Balasubramanian and K. Chennakesavulu, *J. Mater. Chem. A*, 2014, **2**, 15598-15610.
75. M. Mandal, V. Nagaraju, G. V. Karunakar, B. Sarma, B. J. Borah and K. K. Bania, *J. Phys. Chem. C*, 2015, **119**, 28854-28870.
76. M. Sharma, B. Das, G. V. Karunakar, L. Satyanarayana and K. K. Bania, *J. Phys. Chem. C*, 2016, **120**, 13563-13573.
77. R. Ganesan and B. Viswanathan, *J. Phys. Chem. B*, 2004, **108**, 7102-7114.
78. C. A. Bessel and D. R. Rolison, *J. Phys. Chem. B*, 1997, **101**, 1148-1157.
79. W. Turbeville, D. S. Robins and P. K. Dutta, *J. Phys. Chem.*, 1992, **96**, 5024-5029.
80. Y. Umemura, Y. Minai and T. Tominaga, *J. Phys. Chem. B*, 1999, **103**, 647-652.
81. G. Sewell, R. J. Forster and T. E. Keyes, *J. Phys. Chem. A*, 2008, **112**, 880-888.
82. K. K. Bania and R. C. Deka, *J. Phys. Chem. C*, 2011, **115**, 9601-9607.
83. S. Chandra Mohan, D. Bhattacharjee, R. Chandra Deka and K. Jothivenkatachalam, *RSC Adv.*, 2016, **6**, 71214-71222.



This document was created with the Win2PDF "print to PDF" printer available at <http://www.win2pdf.com>

This version of Win2PDF 10 is for evaluation and non-commercial use only.

This page will not be added after purchasing Win2PDF.

<http://www.win2pdf.com/purchase/>